1-1-2019

KIAA1549-BRAF Expression Establishes A Permissive Tumor Microenvironment Through Nfκb-Mediated CCL2 Production

Ran Chen

Chanel Keoni

Christopher A. Waker

Robert M. Lober
Wright State University, robert.lober@wright.edu

Robert M. Lober
Wright State University, robert.lober@wright.edu

See next page for additional authors

NEOPLASIA
www.neoplasia.com

Volume 21 Number 1 January 2019 pp. 52–60 52

KIAA1549-BRAF Expression Establishes a Permissive Tumor Microenvironment Through NFκB-Mediated CCL2 Production

Ran Chen[*], Chanel Keoni[†], Christopher A. Waker[‡], Robert M. Lober[†,‡,§], Yi-Hsien Chen[¶] and David H. Gutmann[*]

[*]Department of Neurology, Washington University, St. Louis, MO; [†]Department of Neurosurgery, Dayton Children's Hospital, One Children's Plaza, Dayton, OH; [‡]Departments of Neuroscience, Cell Biology, and Physiology, Boonshoft School of Medicine, Wright State University, Dayton, OH; [§]Department of Pediatrics, Boonshoft School of Medicine, Wright State University, Dayton, OH; [¶]Washington University School of Medicine, Department of Genetics, St. Louis, 63110, USA

Abstract

KIAA1549-BRAF is the most frequently identified genetic mutation in sporadic pilocytic astrocytoma (PA), creating a fusion BRAF (f-BRAF) protein with increased BRAF activity. *Fusion-BRAF*-expressing neural stem cells (NSCs) exhibit increased cell growth and can generate glioma-like lesions following injection into the cerebella of naïve mice. Increased Iba1^{+} monocyte (microglia) infiltration is associated with murine *f-BRAF*-expressing NSC-induced glioma-like lesion formation, suggesting that *f-BRAF*-expressing NSCs attract microglia to establish a microenvironment supportive of tumorigenesis. Herein, we identify Ccl2 as the chemokine produced by *f-BRAF*-expressing NSCs, which is critical for creating a permissive stroma for gliomagenesis. In addition, f-BRAF regulation of Ccl2 production operates in an ERK- and NFκB-dependent manner in cerebellar NSCs. Finally, Ccr2-mediated microglia recruitment is required for glioma-like lesion formation *in vivo*, as tumor do not form in *Ccr2*-deficient mice following *f-BRAF*-expressing NSC injection. Collectively, these results demonstrate that f-BRAF expression creates a supportive tumor microenvironment through NFκB-mediated Ccl2 production and microglia recruitment.

Neoplasia (2019) 21, 52–60

Introduction

Low-grade gliomas (LGGs) represent the most common central nervous system (CNS) tumor occurring in children, with pilocytic astrocytoma (PAs) being the most frequently encountered benign neoplasm in this age group [1]. The majority of pediatric LGGs are caused by tandem duplications involving the *BRAF* gene (e.g., *KIAA1549:BRAF* rearrangement), which typifies sporadic PAs arising in the cerebellum [2–4]. Based on these observations, we previously demonstrated that ectopic *KIAA1549:BRAF* expression in mouse cerebellar neural stem cells (NSCs) is sufficient to generate glioma-like lesions following implantation in the naïve murine cerebellum [5]. In addition, increased *KIAA1549:BRAF*-driven NSC proliferation is mediated through hyperactivation of the MEK/ERK signaling pathway [5].

Similar to low-grade gliomas arising in children with the Neurofibromatosis type 1 (NF1) cancer predisposition syndrome, these glial tumors are highly dependent on their local microenvironment, and in experimental model systems, are controlled by non-neoplastic stromal cells. Prior studies using *Nf1* genetically engineered mouse strains have revealed that brain monocytes (microglia) are the driving stromal cell type in these tumors, such that their genetic or pharmacologic inhibition attenuates tumor formation and growth [6–8]. Importantly, monocytes can comprise as many as 30–50% of the total number of cells in PAs [9,10]. The presence of these monocytes suggests that the recruitment and activation of microglia and macrophages represent key steps in glioma formation and maintenance.

In order to define the role of microglia in sporadic *KIAA1549:BRAF* (f-BRAF)-driven low-grade glioma, we leveraged converging

Address all correspondence to: David H. Gutmann, MD, PhD, Neurology Department, Washington University School of Medicine, Box 8111, 660 S. Euclid Avenue, St. Louis, MO 63110. E-mail: gutmannd@wustl.edu
Received 20 July 2018; Revised 9 November 2018; Accepted 12 November 2018

1476-5586
https://doi.org/10.1016/j.neo.2018.11.007

in vitro and *in vivo* approaches to demonstrate that *KIAA1549:BRAF* positively regulates cerebellar NSC Ccl2 expression through ERK-dependent NFκB activation. The importance of Ccl2 to tumorigenesis was further underscored by the failure of low-grade glioma-like lesions to form following the implantation of *f-BRAF*-expressing NSCs into *Ccr2*−/− mice.

Materials and Methods

Mice

The *KIAA1549:BRAF* conditional transgenic mouse strain were generated as previously described [11]. $Ccr2^{+/RFP}$ (Keiko Hirose, Washington University) were intercrossed to generate *Ccr2*−/− ($Ccr2^{RFP}/Ccr2^{RFP}$) mice. All mice were maintained on a C57BL/6 background, and used in accordance with an approved Animal Studies protocol at Washington University.

Primary NSC Isolation and Culture

Cerebellar hemispheres were micro-dissected from the brains of postnatal day 2–3 (PN2–3) conditional *f-BRAF* (Lox-STOP-Lox-*KIAA1549:BRAF* transgenic mice [11]) pups to establish primary neural stem cell (NSC) cultures [12]. Control and *f-BRAF*-expressing NSCs were generated following infection with Adenovirus type 5 (Ad5) containing β-galactosidase (Ad5-LacZ) or Cre recombinase (Ad5-Cre) (University of Iowa Gene Transfer Vector Core, Iowa City). Ectopic *f-BRAF* expression in NSCs was also generated through retrovirus infection (Peter Collins, University of Cambridge). The constructs used for retroviral infection were pBABE-puro *KIAA1549:BRAF* and pBABE-puro. *f-BRAF*-expressing cells were confirmed by RNA RT-PCR [13] using the following primer set: 5′ GATGACTTCCTT TCTCGCTGAGGT 3′ and 5′ CTTCCCAGGAAGAGAGGCGA 3′.

Lentivirus Infection

Lentivirus transduction was performed as described previously [14]. Briefly, shRNA-*Ccl2* shRNA-1 (5′ GAATGTGAAGTTGACCCGTAA 3′), shRNA-*Ccl2* shRNA-2 (5′ GAATGGGTCCAGACATACATT 3′), and LacZ shRNA (5′ CCGTCATAGCGATAACGAGTT 3′) in the pLKpuro plasmid were individually co-transfected with pMDLg/pRRE, pRSV-REV and pCMV-VSV-G plasmids into HEK293T cells using the FuGENEHD transfection reagent (Roche). *f-BRAF*-expressing neurospheres (Ad5-Cre-infected *KIAA1549:BRAF* NSCs) were dissociated into single cells by trypsinization, plated on poly-D-lysine- and fibronectin-coated plates, and transduced with virus-containing supernatants from the transduced HEK293T cells. Cells with stable expression of *Ccl2* and *LacZ* siRNA were selected using 0.25 μg/ml puromycin. Transfection was confirmed by RT-PCR.

Intracranial Injections

Four-week-old wild-type C57/BL6 or *Ccr2*-deficient male mice were anesthetized with an intraperitoneal (i.p.) injection of 100 mg/kg ketamine and 6 mg/kg xylazine. NSCs (5×10^5 cells) in 2 μl of PBS were injected into the cerebellum using a Hamilton syringe and a stereotaxic apparatus (coordinates = posterior 5.8 mm from the bregma, lateral 0.7 mm [right], and depth 2.5 mm from dura mater). Mice were euthanized 6 months later.

Immunohistochemistry

Paraffin sections were processed as previously reported [12] prior to staining with appropriate primary antibodies (Supplemental Table 1). Biotinylated secondary antibodies (Vector Laboratories) were used in combination with Vectastain Elite ABC development and hematoxylin counterstaining.

Real-Time qRT-PCR

RNA was purified using the RNeasy Plus Mini Kit (Qiagen) prior to treatment with (10 U) DNase I recombinase (Roche). The DNase was then heat inactivated with EDTA chelation. RNA was reverse transcribed into cDNA using the Omniscript RT kit (Qiagen). Real-time qRT-PCR was performed as previously described [15] using mouse-or human-specific primers (Supplemental Table 2). For each gene, the ΔΔCT values were calculated, where *H3f3a* (or *H3F3A* for human specimens) was used as an internal control. Chemokines and Receptors RT^2 profiler PCR array (PAMM-022Z; Qiagen) analyses were performed according to the manufacturer's recommendations.

Human Pilocytic Astrocytoma (PA) Cell Lines

Following Institutional Review Board approval (Protocol #2016–014), tumor specimens were procured by C.K. and C.A.W. during standard surgical resection by R.M.L. at Dayton Children's Hospital, after necessary tissues were submitted for pathologic diagnosis. Parental consent and, when applicable, patient assent was obtained prior to collection. Fresh tissues for culture were prepared as 50 to 200-mg specimens, placed directly into culture medium consisting of Dulbecco's Minimum Essential Media with F12, 10% heat-inactivated fetal bovine serum (FBS), and 100 μg/ml Primocin™ (Invivogen, Inc.), and transported on wet ice to a sterile hood. Tumors were minced and digested with trypsin and collagenase IV at 37 ° C for 30 minutes, and then inactivated with FBS. Cells were then centrifuged at 1000 rpm for 3 minutes, resuspended in culture medium, and added to 100-mm tissue culture plates. Adherent cells were passaged when 70–80% confluent. Prior to transport, cells were removed with trypsin digestion, followed by FBS inactivation, and centrifuged at 1000 rpm for 3 minutes. Cell pellets were shipped on dry ice to Washington University for further processing and analysis. Clinical and *BRAF* mutation information is included in Supplemental Table S3. Normal human astrocytes (NHA cells; ScienCell Research Laboratories, Inc.) were grown according to the manufacturer's recommendations.

Western Blotting

Cell pellets were lysed in RIPA lysis buffer supplemented with proteinase and phosphatase inhibitors. Protein samples were separated by SDS-PAGE, and then transferred onto Immobilon membranes. Membranes were blocked in Tris-buffered saline 0.1% Tween 20 (TBST) with 5% non-fat dry milk, and incubated with the primary antibodies listed in Supplemental Table 1. Antibodies were diluted in blocking buffer or 5% BSA TBST overnight at 4°C, and horseradish peroxidase conjugated secondary antibodies were added for 1 hour at room temperature prior to chemiluminescence development.

ELISA

Conditioned medium (CM), was collected from control and *f-BRAF*-expressing NSCs, and the levels of CCL2 determined using the Mouse/Rat or Human CCL2/JE/MCP-1 Quantikine ELISA kit (R&D). The number of cells were counted for each condition and used for normalization.

Results and Discussion

Since increased monocyte (microglia and macrophage) infiltration is associated with *f-BRAF*-expressing pilocytic astrocytomas in children [7,9,16] and *f-BRAF*-expressing NSC glioma-like lesion formation in

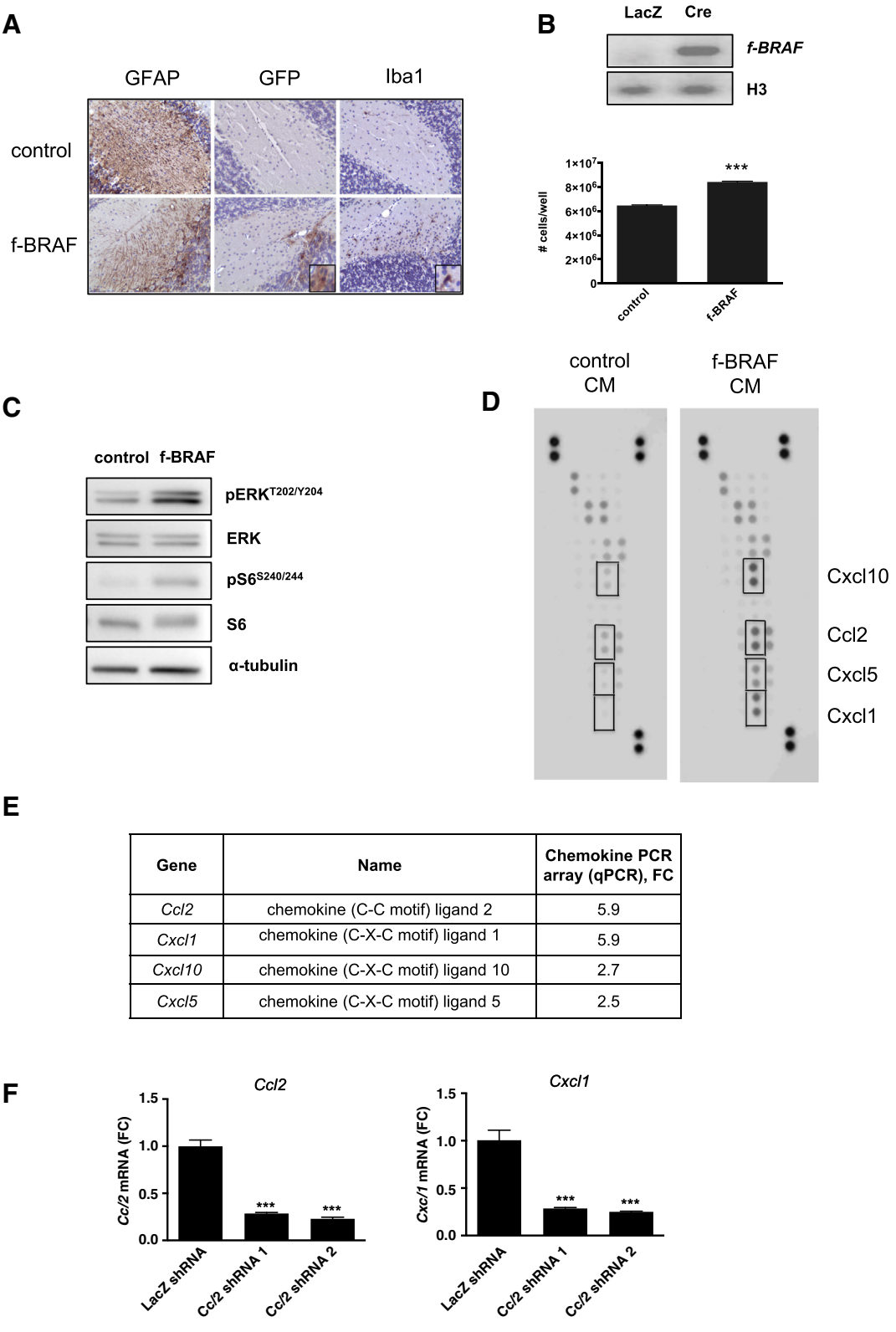

Gene	Name	Chemokine PCR array (qPCR), FC
Ccl2	chemokine (C-C motif) ligand 2	5.9
Cxcl1	chemokine (C-X-C motif) ligand 1	5.9
Cxcl10	chemokine (C-X-C motif) ligand 10	2.7
Cxcl5	chemokine (C-X-C motif) ligand 5	2.5

Figure 1. *f-BRAF*-expressing cerebellar NSCs produce Ccl2. (**A**) GFAP-immunoreactive cells are present at the injection sites of control and *f-BRAF* NSC-injected wild-type mice. Injected sites with tumors also contain GFP-positive *f-BRAF*-expressing cells. Increased Iba1$^+$ cells were detected in *f-BRAF*-induced lesions. (**B**) *f-BRAF* transgene expression was confirmed by RT-PCR in *KIAA1549:BRAF* cerebellar NSCs infected with Ad5-Cre. *f-BRAF*-expressing cerebellar NSCs have increased proliferation relative to controls. (**C**) Increased ERK and S6 phosphorylation was observed following *f-BRAF* expression in cerebellar NSCs. (**D**) Chemokine antibody array revealed increased Cxcl10, Ccl2, Cxcl1 and Cxcl5 expression in the culture medium (CM) of *f-BRAF*-expressing cerebellar NSCs relative to controls. Boxes denote the increased candidate chemokines. (**E**) Quantitative analysis of increased chemokines in *f-BRAF*-expressing cerebellar NSCs using a chemokine PCR array. The mRNA level fold change (FC) for the indicated chemokines are shown in the Table. (**F**) *Ccl2* knockdown using two independently generated *Ccl2* shRNAs demonstrates decreased *Ccl2* mRNA in *f-BRAF*-expressing cerebellar NSCs (**left**). *Cxcl10* mRNA levels were decreased in *Ccl2* knockdown *f-BRAF*-expressing cerebellar NSCs (**right**).

mice [5], we sought to determine whether *f-BRAF* induces chemokine expression to recruit Iba1$^+$ monocytes to the tumor site (Figure 1*A*). To induce *f-BRAF* expression in the presumed cells of origin for cerebellar low-grade glioma, primary cerebellar NSCs were generated from PN2 conditional knock-in *KIAA1549:BRAF* (f-BRAF) mice [11]. Following adenovirus infection, *f-BRAF* expression was only induced in Ad5-Cre-infected NSCs, but not in control Ad5-LacZ-infected cerebellar NSCs (Figure 1*B*). Similar results were also obtained following infection with a retrovirus containing the *KIAA1549:BRAF* transgene (data not shown), and these two approaches were used interchangeably. Similar to our previous studies using these methods [5,11], *f-BRAF*-expressing cerebellar NSCs exhibited elevated ERK activation (ERK$^{Thr202/Tyr204}$ phosphorylation) and increased phosphorylation (activation) of ribosomal S6 protein (Ser$^{240/244}$) (Figure 1*C*). In addition, *f-BRAF*-expressing cerebellum NSCs proliferated faster than infected controls (Figure 1*B*). Consistent with previous reports [5,11,17–19], f-BRAF induces low-grade glioma formation and growth through increased activation of B-RAF downstream effectors, including MEK/ERK and mTOR.

To identify potential chemokines produced by *f-BRAF*-expressing cerebellar NSCs, we employed a commercial chemokine protein array. Since chemokines are typically secreted paracrine factors, we used conditioned medium (CM) from *f-BRAF*-expressing and wild type cerebellar (control) NSCs (Figure 1*D*). In addition, we analyzed chemokine mRNA expression using a commercial RT profiler PCR array (Figure 1*E*). Using both methods, four potential chemokines were identified (Cxcl1, Cxcl5, Cxcl10, Ccl2) at the protein and mRNA levels. However, only Ccl2 and Cxcl1 exhibited >3-fold increases. For this reason, we focused on Ccl2 and Cxcl1.

First, we sought to determine whether Ccl2 regulated Cxcl1 expression, and therefore functioned as the key chemokine to regulate monocyte attraction. By using two independently generated *Ccl2* shRNA constructs, we found that *Ccl2* knockdown reduced *Cxcl1* expression in *f-BRAF*-expressing cerebellar NSCs (Figure 1*F*), thus positioning Ccl2 as the master regulator worthy of further investigation.

Second, we leveraged the online NCBI GEO database, which contains two separate gene expression profiles from human PAs and normal brain samples (GSE42656 and GSE44971). GSE42656 contains 14 PAs and 4 fetal brain controls, whereas GSE44971 has 35 cerebellar PAs and 9 normal cerebellum samples. In both datasets, *CCL2* levels were elevated in the PAs relative to their non-neoplastic counterparts (Figure 2*A*). In addition, since the fusion BRAF rearrangement is a genomic hallmark of optic pathway and cerebellar PAs [3,20], we compared cerebellar PAs to non-neoplastic cerebellar tissue in the GSE44971 dataset, and similarly observed increased *CCL2* expression in the tumors (Figure 2*B*). Moreover, we obtained three short-term primary human PA cell lines established from fresh surgical specimens, and analyzed them for *CCL2* mRNA expression. *CCL2* mRNA was increased in all 3 PA cell lines relative to normal human astrocytes (Figure 2*C*), demonstrating that the tumor cells produce CCL2. Third, Ccl2 expression was increased four-fold in independently-isolated *f-BRAF*-expressing cerebellar NSCs at the protein level (ELISA) (Figure 2*D*), whereas in cortical NSCs and cerebellar astrocytes, which do not increase their proliferation in response to f-BRAF, did not (Figure 2*E*). In this regard, previous studies have revealed that *f-BRAF* expression has both tissue- and cell-type specific effects: Whereas f-BRAF induces mTOR activation and increased cell growth in brainstem and cerebellar NSCs, no increase in mTOR activation or cell proliferation was observed when *f-BRAF* was expressed in cerebellar astrocytes or cortical NSCs [5,13]. These latter results indicate that the patterning of gliomagenesis is partly dictated by the specific cell of origin (cell type and brain region) [13,14].

Taken together, based on these converging mouse and human data, we sought to focus on Ccl2 as an *f-BRAF*-regulated chemokine potentially important for recruiting microglia to establish a permissive tumor microenvironment. CCL2 has been previously implicated in tumorigenesis and metastasis in several other solid tumor types [21,22], including high-grade glioma [23,24]. As such, malignant glioma cells elaborate chemoattractants, including CCL2, that promote the directional migration of macrophages and microglia to the developing tumor bed [25–29]. In addition, a correlation between glioma grade and tumor microglia/macrophage content has been demonstrated [30]. However, the role of CCL2 in PA tumorigenesis has not been investigated.

To determine whether Ccl2 is regulated by BRAF-mediated ERK activation, control and *f-BRAF*-expressing cerebellar NSCs were treated with two different MEK inhibitors, PD0325901 (PD901) and Trametinib, each resulting in decreased ERK activation (Thr$^{202/Tyr204}$ phosphorylation; Figure 3*A*). Following either PD901 or Trametinib treatment, *Ccl2* mRNA level and protein levels were reduced (Figure 3, *B* and *C*), indicating that Ccl2 is regulated by the BRAF-MEK–ERK signaling pathway, consistent with the known function of f-BRAF in MEK/ERK activation [5,11,17–19].

Ccl2 gene expression is transcriptionally controlled at the promoter level by several different transcriptional regulators, including NFκB, C/EBP1, AP-1 and SP-1 [31]. Since NFκB is an important transcription factor for *CCL2* regulation in glial cells [32], we sought to determine whether BRAF-MEK–ERK mediates Ccl2 induction through NFκB activation. NFκB activation is partly regulated through IκB phosphorylation, where the inactive cytosolic form of NFκB becomes associated with IκB$_\alpha$. Following IκB$_\alpha$ phosphorylation, the NFκB heterodimer dissociates from IκB$_\alpha$ and enters the nucleus in its active form. As shown in Figure 3*D*, IκB$_\alpha$ phosphorylation (NFκB activation) is increased in *f-BRAF*-expressing cerebellar NSCs, and MEK inhibition leads to reduced IκB$_\alpha$ phosphorylation (Ser^{32}) levels. Lastly, to demonstrate that NFκB activation is responsible for *f-BRAF*-mediated Ccl2 induction, *f-BRAF*-expressing cerebellar NSCs were treated with TPCA-1, a selective inhibitor of IκB$_\alpha$ kinase that inhibits NF-κB nuclear localization. *f-BRAF*-expressing NSCs treated with TPCA-1 showed reduced IκB$_\alpha$ phosphorylation (Ser^{32}) level and decreased *Ccl2* mRNA expression (Figure 3*E*), thus establishing that f-BRAF regulates Ccl2 expression in a MEK/NFκB-dependent manner. The finding that Ccl2 induction following *f-BRAF* expression in cerebellar NSCs involves MEK/ERK-dependent IκB kinase and NFκB activation is consistent with previous reports in other cell types (macrophages), where lipopolysaccharide (LPS)-induced NFκB activation is dependent upon ERK activation through the prevention of activate IκB kinase degradation [33]. In addition, MEK/ERK signaling pathway activation is similarly important for TNFα-induced CCL2 expression in human proximal tubular epithelial cells [34].

Since Ccl2 could potentially function in an autocrine manner, as previously reported for CXCL12 and CCL5 [35,36], we sought to determine whether Ccl2 could promote *f-BRAF*-expressing cerebellar NSC growth. Because Ccl2 can act through its receptors, Ccr2 and Ccr4, to increase NSC growth, we first examined *Ccl2* receptor expression, and found that cerebellar NSCs express only the *Ccr4* receptor (Figure 4*A*). Second, we added recombinant mouse Ccl2 (200 ng /ml) to control and *f-BRAF*-expressing cerebellar NSCs, but observed no significant increase in proliferation (Figure 4*B*). Third, we assessed the effect of *Ccl2* silencing on *f-BRAF*-expressing NSC

A

Gene	Fold Change (PA: normal) (GSE42656)	p	Fold Change (PA: normal) (GSE44971)	p
CCL2	7.64	6.91e-5	1.83	1.22e-9
CXCL1	-0.96	4.35 e-1(n.s.)	-0.82	1.26 e-2 (n.s.)
CXCL5	-0.88	1.64 e-2(n.s.)	-0.59	9.91 e-2 (n.s.)
CXCL10	1.12	2.64 e-1(n.s.)	1.11	3.06 e-2 (n.s.)

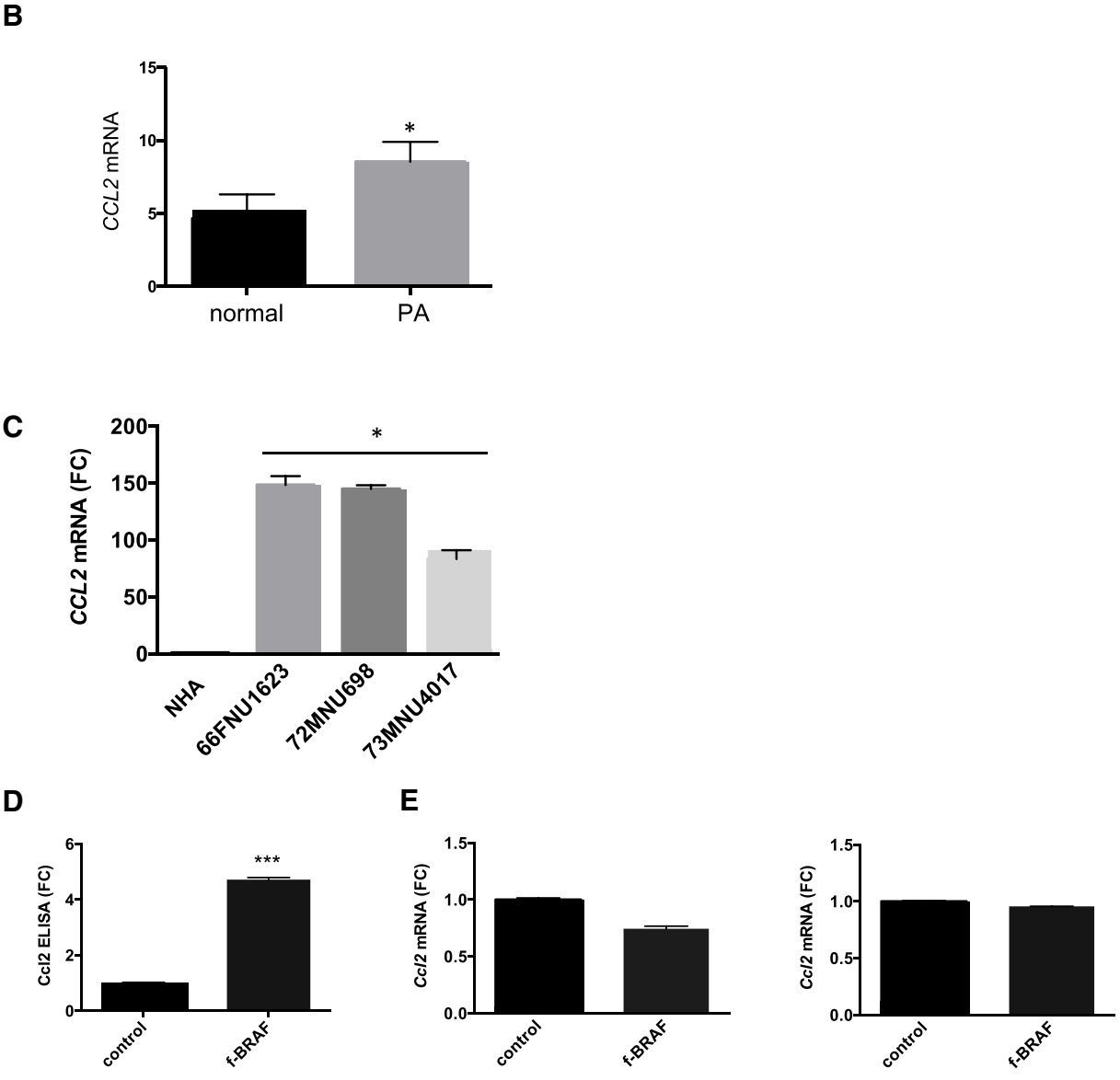

Figure 2. Human and mouse low-grade glioma cells produce CCL2. (**A**) Microarray analysis of *CCL2*, *CXCL1*, *CXCL5* and *CXCL10* mRNA levels in two different human PA datasets (GSE42565 and GSE44971), comparing PAs and control non-neoplastic brain samples, displayed as fold changes with p-values. (**B**) Microarray analysis containing only cerebellar PA tumors and non-neoplastic cerebellar tissue (GSE44971 dataset) reveals increased *CCL2* expression in the tumors. (**C**) Increased *CCL2* mRNA expression is observed in three primary human PA tumors relative to normal human astrocyte (NHA) controls. Data are expressed as fold changes relative to the normal human astrocytes. (**D**) *f-BRAF*-expressing cerebellar NSCs express more Ccl2 protein as measured by ELISA. (**E**) Cortex NSCs (**left**) and cerebellum astrocytes (**right**) expressing *f-BRAF* show no increase in *Ccl2* mRNA expression. Error bars denote mean ± SD. (*) $P < .05$, (***) $P < .001$.

proliferation. shRNA-mediated *Ccl2* knockdown using two independently derived shRNA constructs had no effect on *f-BRAF*-expressing cerebellar NSC proliferation (Figure 4*C*). Taken together, Ccl2 does not increase *f-BRAF*-expressing cerebellar NSC growth, suggesting that its primary effect is paracrine, as previously shown for human malignant glioma cell lines [37].

To determine whether CCL2 was responsible for microglia infiltration and glioma-like lesion formation *in vivo*, *f-BRAF*-

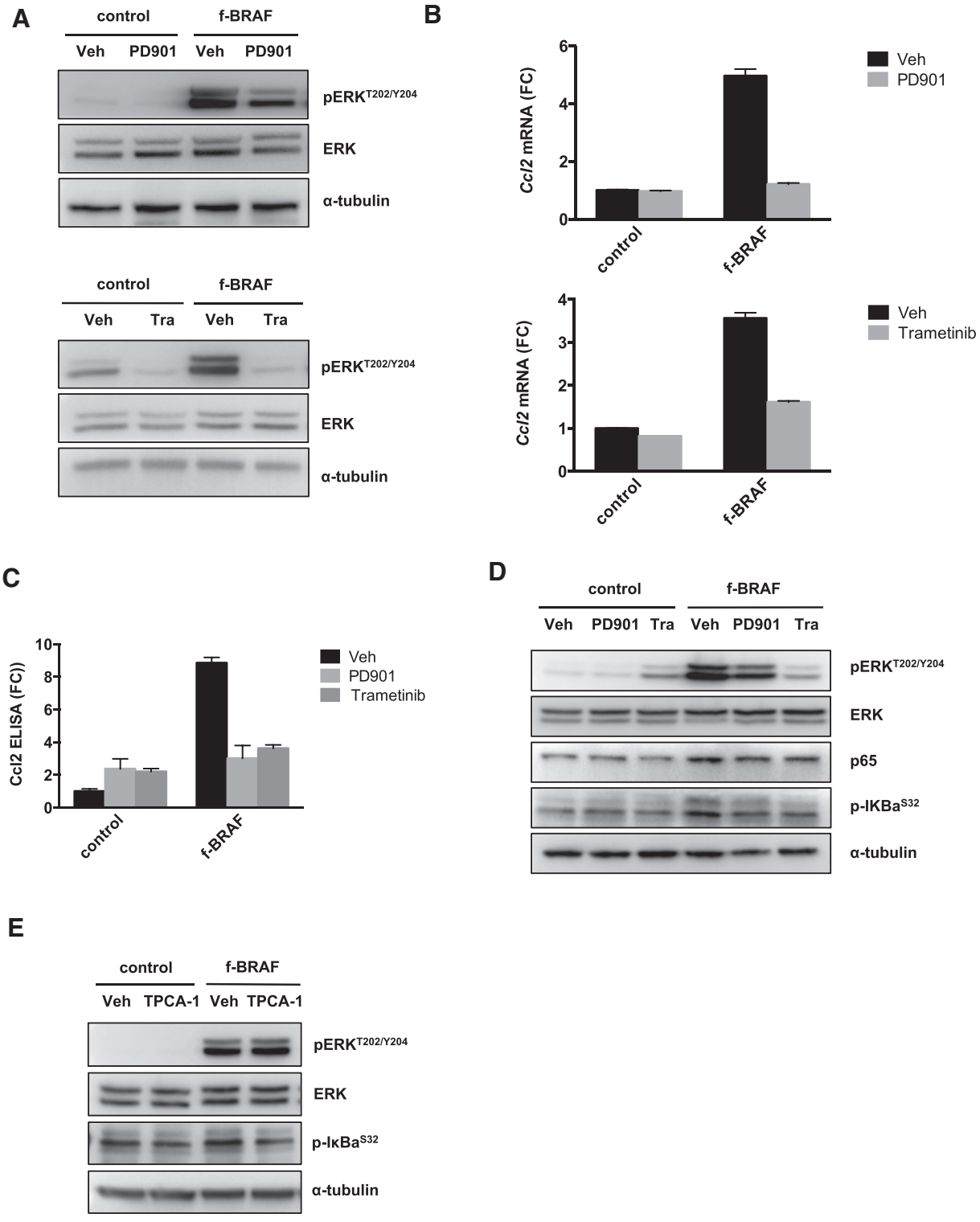

Figure 3. Increased Ccl2 by f-BRAF is mediated by MEK–ERK-NFκB activation. (**A**) Increased ERK phosphorylation in *f-BRAF*-expressing cerebellar NSCs was attenuated following treatment with 10 nM PD0325901 (PD901; **top**) or 50 nM Trametinib (Tra; **bottom**). α-tubulin is an internal protein loading control. Veh, Vehicle. (**B**) Increased *Ccl2* mRNA levels in *f-BRAF*-expressing cerebellar NSCs were reduced to control cells levels following treatment with PD901 (**top**) or Trametinib (Tra; **bottom**). (**C**) Increased Ccl2 protein levels in *f-BRAF*-expressing cerebellar NSCs were reduced to control levels following PD901 or Trametinib treatment as measured by ELISA. (**D**) Phospho-IκB (Ser^{32}) was decreased in *f-BRAF*-expressing cerebellar NSCs following PD901 or Tra treatment. (**E**) The increased phospho-IκB$_{\alpha}$ (Ser^{32}) in *f-BRAF*-expressing cerebellar NSCs was decreased following treatment with 500 nm TPCA-1. Increased *Ccl2* mRNA level in *f-BRAF*-expressing cerebellar NSCs was reduced to control cell levels following TPCA-1 treatment.

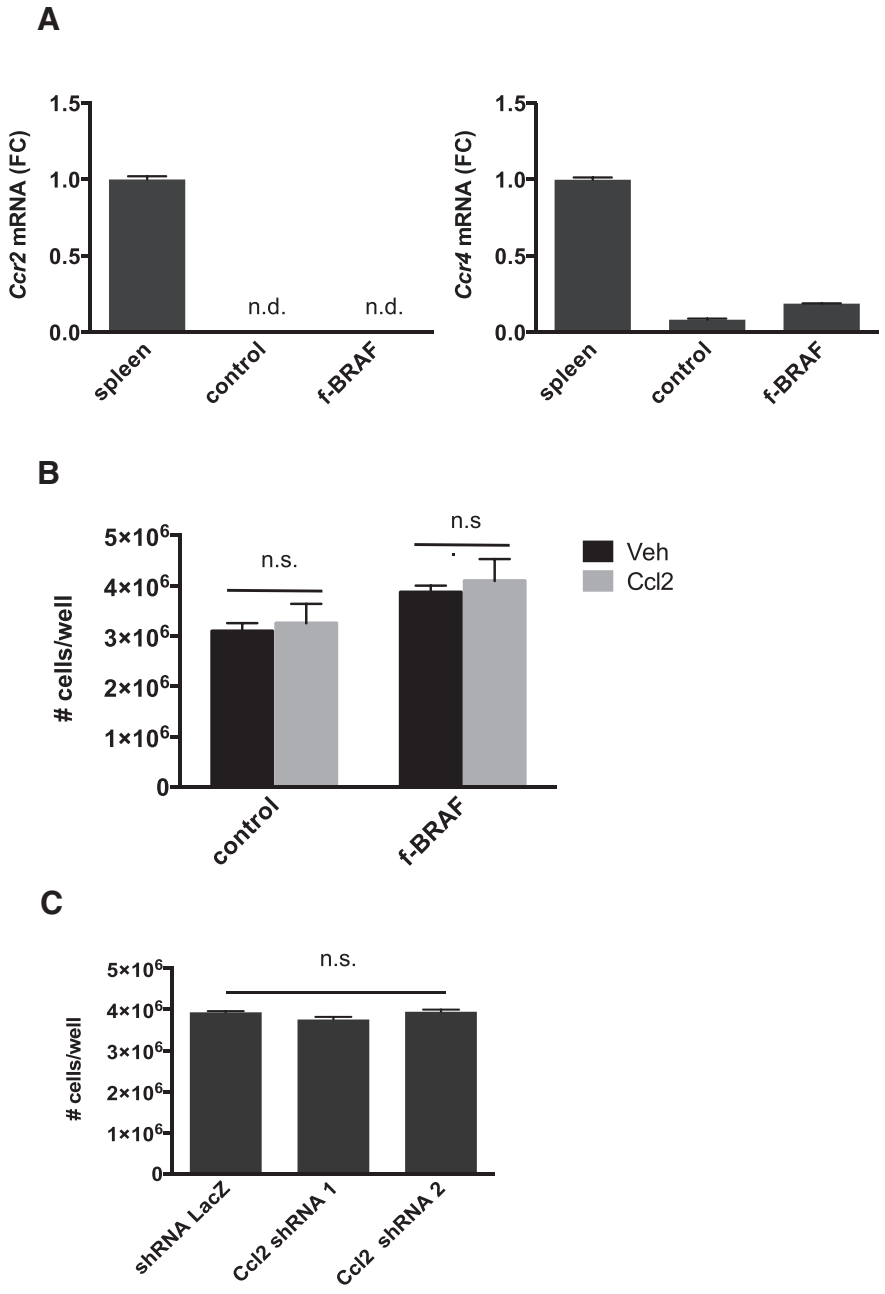

Figure 4. Ccl2 does not function in an autocrine manner to increase cerebellar NSC growth. (**A**) *Ccr4*, but not *Ccr2*, mRNA was detected in cerebellar NSCs. (**B**) Recombinant Ccl2 protein did not increase control or f *f-BRAF*-expressing cerebellar NSC proliferation. (**C**) *Ccl2* knockdown in *f-BRAF*-expressing cerebellar NSCs had no effect on cell proliferation.

expressing cerebellar NSCs were injected into the cerebella of 4-week-old wild type and *Ccr2*-deficient mice ($Ccr2^{RFP}/Ccr2^{RFP}$ mice). Using this method, low-grade glioma-like form between 3 and 6 months after the injection of *f-BRAF*-expressing cerebellar NSCs. In striking contrast, no tumors form in mice engrafted with wild type (control) cerebellar NSCs. However, in both cases, the injection site exhibited increased glial fibrillary acid protein (GFAP) immunoreactivity, thus enabling the identification of the site of injection in each mouse (Figure 5). Since *f-BRAF*-expressing NSCs express green fluorescent protein (GFP), GFP^+ cells were only identified at the injection sites of f-BRAF NSCs-transplanted mice. Consistent with our previous study, at 6 months post-injection, *f-BRAF*-expressing NSC-engrafted wild type mice (n = 5) had increased numbers of proliferating ($Ki67^+$) cells and increased microglia ($Iba1^+$ cells) infiltration relative to control NSC-injected wild type mice (n = 5) (Figure 5). In striking contrast, *Ccr2*-deficient mice bearing *f-BRAF*-expressing NSCs (n = 5) showed reduced numbers of proliferating cells and microglia infiltration relative to wild-type mice. Given the absence of an autocrine effect, these results indicate that Ccl2 establishes a supportive microenvironment for gliomagenesis through Ccr2-mediated microglia recruitment.

The importance of microglia and macrophages to glioma formation, growth and invasion is further underscored by several studies in which pharmacologic or genetic silencing of microglia/macrophage function attenuates malignant glioma growth [27,38–40]. Moreover, in *Nf1* mouse models of low-grade glioma,

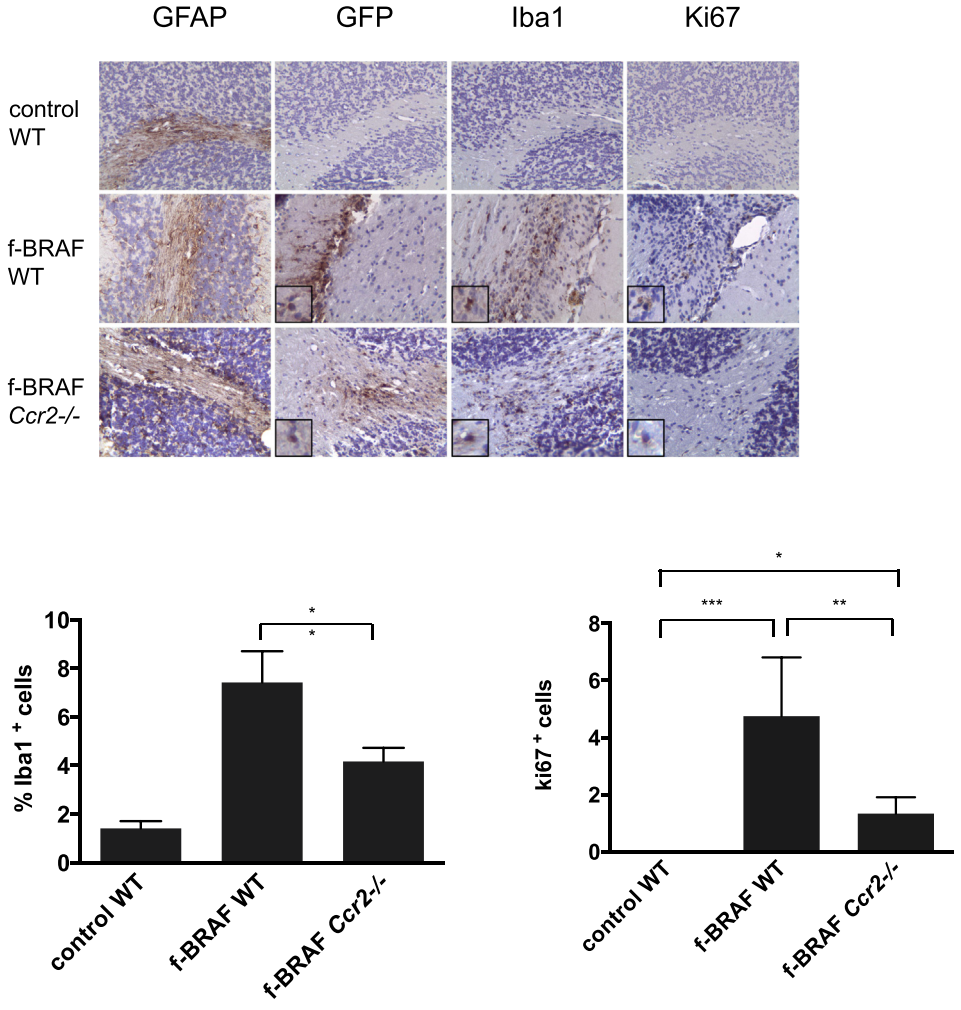

Figure 5. Ccr2 is required for microglia infiltration and glioma-like lesion formation *in vivo*. GFAP-immunoreactive cells were detected at the injection sites of control and *f-BRAF*-expressing cerebellar NSC-injected mice. GFP$^+$ cells were only detected in *f-BRAF*-expressing cerebellar NSC-injected mice. Increased Iba1$^+$ cells (microglia) and Ki67$^+$ (proliferating) cells were observed in *f-BRAF*-expressing cerebellar NSC-induced glioma-like lesions in wild type mice. The numbers of Ki67$^+$ and Iba1$^+$ cells were attenuated when *f-BRAF*-expressing cerebellar NSCs were injected into *Ccr2*-deficient mice. Error bars denote mean ± SD. (*) $P < .05$; (**) $P < .01$; (***) $P < .001$.

we have previously shown that microglia are critical for glioma formation and growth [6,8,41] through the elaboration of key chemokines [35], specifically Ccl5 [42].

While the mechanism underlying microglia support of *KIAA1549:BRAF*-associated low-grade glioma growth remains to be elucidated, we have excluded numerous chemokines previously implicated in *Nf1* mouse low-grade glioma pathogenesis, including Ccl5 and Cxcl12 (data not shown). Future investigations will be required to identify the responsive microglia-produced growth factors that support sporadic low-grade glioma growth. Nonetheless, in the current study, we establish that Ccl2 is the major chemokine produced by *KIAA1549:BRAF*-expressing NSCs important for low-grade glioma-like lesion formation in mice. In addition to demonstrating the molecular mechanism responsible for MEK-driven Ccl2 transcription, we demonstrate that Ccr2 is required for both microglia infiltration and low-grade glioma-like lesion formation *in vivo*. Collectively, these findings reveal how the frequently reported PA genetic alteration, *KIAA1549:BRAF* creates a permissive low-grade glioma microenvironment in a paracrine fashion through the Ccl2/Ccr2 axis.

Supplementary data to this article can be found online at https://doi.org/10.1016/j.neo.2018.11.007.

Acknowledgements

We appreciate the technical assistance provided by Courtney Corman during the execution of these experiments. This work was funded unrestricted funds from Schnuck Markets, Inc. and a Research Program Award from the National Institute of Neurological Disorders and Stroke (1-R35-NS07211-01 to D.H.G.). The Living Biobank at Dayton Children's Hospital is supported by a generous grant from the Gala of Hope Foundation.

References

[1] Dolecek TA, Propp JM, Stroup NE, and Kruchko C (2012). CBTRUS statistical report: primary brain and central nervous system tumors diagnosed in the United States in 2005-2009. *Neuro-Oncology* **14**(Suppl. 5), v1–49.

[2] Pfister S, Janzarik WG, Remke M, Ernst A, Werft W, and Becker N, et al (2008). BRAF gene duplication constitutes a mechanism of MAPK pathway activation in low-grade astrocytomas. *J Clin Invest* **118**(5), 1739–1749.

[3] Yu J, Deshmukh H, Gutmann RJ, Emnett RJ, Rodriguez FJ, and Watson MA, et al (2009). Alterations of BRAF and HIPK2 loci predominate in sporadic pilocytic astrocytoma. *Neurology* **73**(19), 1526–1531.

[4] Jones DT, Kocialkowski S, Liu L, Pearson DM, Backlund LM, and Ichimura K, et al (2008). Tandem duplication producing a novel oncogenic BRAF fusion gene defines the majority of pilocytic astrocytomas. *Cancer Res* **68**(21), 8673–8677.

[5] Kaul A, Chen YH, Emnett RJ, Dahiya S, and Gutmann DH (2012). Pediatric glioma-associated KIAA1549:BRAF expression regulates neuroglial cell growth in a cell type-specific and mTOR-dependent manner. *Genes Dev* **26**(23), 2561–2566.

[6] Daginakatte GC and Gutmann DH (2007). Neurofibromatosis-1 (Nf1) heterozygous brain microglia elaborate paracrine factors that promote Nf1-deficient astrocyte and glioma growth. *Hum Mol Genet* **16**(9), 1098–1112.

[7] Simmons GW, Pong WW, Emnett RJ, White CR, Gianino SM, and Rodriguez FJ, et al (2011). Neurofibromatosis-1 heterozygosity increases microglia in a spatially and temporally restricted pattern relevant to mouse optic glioma formation and growth. *J Neuropathol Exp Neurol* **70**(1), 51–62.

[8] Pong WW, Higer SB, Gianino SM, Emnett RJ, and Gutmann DH (2013). Reduced microglial CX3CR1 expression delays neurofibromatosis-1 glioma formation. *Ann Neurol* **73**(2), 303–308.

[9] Tanaka Y, Sasaki A, Ishiuchi S, and Nakazato Y (2008). Diversity of glial cell components in pilocytic astrocytoma. *Neuropathology* **28**(4), 399–407.

[10] Klein R and Roggendorf W (2001). Increased microglia proliferation separates pilocytic astrocytomas from diffuse astrocytomas: a double labeling study. *Acta Neuropathol* **101**(3), 245–248.

[11] Kaul A, Chen YH, Emnett RJ, Gianino SM, and Gutmann DH (2013). Conditional KIAA1549:BRAF mice reveal brain region- and cell type-specific effects. *Genesis* **51**(10), 708–716.

[12] Dasgupta B and Gutmann DH (2005). Neurofibromin regulates neural stem cell proliferation, survival, and astroglial differentiation in vitro and in vivo. *J Neurosci* **25**(23), 5584–5594.

[13] Lee DY, Gianino SM, and Gutmann DH (2012). Innate neural stem cell heterogeneity determines the patterning of glioma formation in children. *Cancer Cell* **22**(1), 131–138.

[14] Lee DY, Yeh TH, Emnett RJ, White CR, and Gutmann DH (2010). Neurofibromatosis-1 regulates neuroglial progenitor proliferation and glial differentiation in a brain region-specific manner. *Genes Dev* **24**(20), 2317–2329.

[15] Yeh TH, Lee DY, Gianino SM, and Gutmann DH (2009). Microarray analyses reveal regional astrocyte heterogeneity with implications for neurofibromatosis type 1 (NF1)-regulated glial proliferation. *Glia* **57**(11), 1239–1249.

[16] AlShakweer W, Alwelaie Y, Mankung AM, and Graeber MB (2011). Bone marrow-derived microglia in pilocytic astrocytoma. *Front Biosci (Elite Ed)* **3**, 371–379.

[17] Forshew T, Tatevossian RG, Lawson AR, Ma J, Neale G, and Ogunkolade BW, et al (2009). Activation of the ERK/MAPK pathway: a signature genetic defect in posterior fossa pilocytic astrocytomas. *J Pathol* **218**(2), 172–181.

[18] Gronych J, Korshunov A, Bageritz J, Milde T, Jugold M, and Hambardzumyan D, et al (2011). An activated mutant BRAF kinase domain is sufficient to induce pilocytic astrocytoma in mice. *J Clin Invest* **121**(4), 1344–1348.

[19] Jones DT, Gronych J, Lichter P, Witt O, and Pfister SM (2012). MAPK pathway activation in pilocytic astrocytoma. *Cell Mol Life Sci* **69**(11), 1799–1811.

[20] Jacob K, Albrecht S, Sollier C, Faury D, Sader E, and Montpetit A, et al (2009). Duplication of 7q34 is specific to juvenile pilocytic astrocytomas and a hallmark of cerebellar and optic pathway tumours. *Br J Cancer* **101**(4), 722–733.

[21] Kitamura T, Qian BZ, Soong D, Cassetta L, Noy R, and Sugano G, et al (2015). CCL2-induced chemokine cascade promotes breast cancer metastasis by enhancing retention of metastasis-associated macrophages. *J Exp Med* **212**(7), 1043–1059.

[22] Chun E, Lavoie S, Michaud M, Gallini CA, Kim J, and Soucy G, et al (2015). CCL2 Promotes Colorectal Carcinogenesis by Enhancing Polymorphonuclear Myeloid-Derived Suppressor Cell Population and Function. *Cell Rep* **12**(2), 244–257.

[23] Desbaillets I, Tada M, de Tribolet N, Diserens AC, Hamou MF, and Van Meir EG (1994). Human astrocytomas and glioblastomas express monocyte chemoattractant protein-1 (MCP-1) in vivo and in vitro. *Int J Cancer* **58**(2), 240–247.

[24] Graves DT, Jiang YL, Williamson MJ, and Valente AJ (1989). Identification of monocyte chemotactic activity produced by malignant cells. *Science* **245**(4925), 1490–1493.

[25] Platten M, Kretz A, Naumann U, Aulwurm S, Egashira K, and Isenmann S, et al (2003). Monocyte chemoattractant protein-1 increases microglial infiltration and aggressiveness of gliomas. *Ann Neurol* **54**(3), 388–392.

[26] Held-Feindt J, Hattermann K, Muerkoster SS, Wedderkopp H, Knerlich-Lukoschus F, and Ungefroren H, et al (2010). CX3CR1 promotes recruitment of human glioma-infiltrating microglia/macrophages (GIMs). *Exp Cell Res* **316**(9), 1553–1566.

[27] Pyonteck SM, Akkari L, Schuhmacher AJ, Bowman RL, Sevenich L, and Quail DF, et al (2013). CSF-1R inhibition alters macrophage polarization and blocks glioma progression. *Nat Med* **19**(10), 1264–1272.

[28] Ryder M, Gild M, Hohl TM, Pamer E, Knauf J, and Ghossein R, et al (2013). Genetic and pharmacological targeting of CSF-1/CSF-1R inhibits tumor-associated macrophages and impairs BRAF-induced thyroid cancer progression. *PLoS One* **8**(1)e54302.

[29] Leung SY, Wong MP, Chung LP, Chan AS, and Yuen ST (1997). Monocyte chemoattractant protein-1 expression and macrophage infiltration in gliomas. *Acta Neuropathol* **93**(5), 518–527.

[30] Roggendorf W, Strupp S, and Paulus W (1996). Distribution and characterization of microglia/macrophages in human brain tumors. *Acta Neuropathol* **92**(3), 288–293.

[31] Yadav A, Saini V, and Arora S (2010). MCP-1: chemoattractant with a role beyond immunity: a review. *Clin Chim Acta* **411**(21–22), 1570–1579.

[32] Thompson WL and Van Eldik LJ (2009). Inflammatory cytokines stimulate the chemokines CCL2/MCP-1 and CCL7/MCP-3 through NFkB and MAPK dependent pathways in rat astrocytes [corrected]. *Brain Res* **1287**, 47–57.

[33] Chen BC and Lin WW (2001). PKC- and ERK-dependent activation of I kappa B kinase by lipopolysaccharide in macrophages: enhancement by P2Y receptor-mediated CaMK activation. *Br J Pharmacol* **134**(5), 1055–1065.

[34] Ho AW, Wong CK, and Lam CW (2008). Tumor necrosis factor-alpha up-regulates the expression of CCL2 and adhesion molecules of human proximal tubular epithelial cells through MAPK signaling pathways. *Immunobiology* **213**(7), 533–544.

[35] Warrington NM, Woerner BM, Daginakatte GC, Dasgupta B, Perry A, and Gutmann DH, et al (2007). Spatiotemporal differences in CXCL12 expression and cyclic AMP underlie the unique pattern of optic glioma growth in neurofibromatosis type 1. *Cancer Res* **67**(18), 8588–8595.

[36] Pan Y, Smithson LJ, Ma Y, Hambardzumyan D, and Gutmann DH (2017). Ccl5 establishes an autocrine high-grade glioma growth regulatory circuit critical for mesenchymal glioblastoma survival. *Oncotarget* **8**(20), 32977–32989.

[37] Zhang J, Sarkar S, Cua R, Zhou Y, Hader W, and Yong VW (2012). A dialog between glioma and microglia that promotes tumor invasiveness through the CCL2/CCR2/interleukin-6 axis. *Carcinogenesis* **33**(2), 312–319.

[38] Sarkar S, Doring A, Zemp FJ, Silva C, Lun X, and Wang X, et al (2014). Therapeutic activation of macrophages and microglia to suppress brain tumor-initiating cells. *Nat Neurosci* **17**(1), 46–55.

[39] Sadahiro H, Kang KD, Gibson JT, Minata M, Yu H, and Shi J, et al (2018). Activation of the Receptor Tyrosine Kinase AXL Regulates the Immune Microenvironment in Glioblastoma. *Cancer Res* **78**(11), 3002–3013.

[40] Chen Z, Feng X, Herting CJ, Garcia VA, Nie K, and Pong WW, et al (2017). Cellular and Molecular Identity of Tumor-Associated Macrophages in Glioblastoma. *Cancer Res* **77**(9), 2266–2278.

[41] Daginakatte GC, Gianino SM, Zhao NW, Parsadanian AS, and Gutmann DH (2008). Increased c-Jun-NH2-kinase signaling in neurofibromatosis-1 heterozygous microglia drives microglia activation and promotes optic glioma proliferation. *Cancer Res* **68**(24), 10358–10366.

[42] Solga AC, Pong WW, Kim KY, Cimino PJ, Toonen JA, and Walker J, et al (2015). RNA Sequencing of Tumor-Associated Microglia Reveals Ccl5 as a Stromal Chemokine Critical for Neurofibromatosis-1 Glioma Growth. *Neoplasia* **17**(10), 776–788.